

Predicted high-temperature superconductivity in rare earth hydride ErH₂ at moderate pressure

Yiding Liu,^{1,2} Qiang Fan,³ Jianhui Yang,¹ Lili Wang,⁴ Weibin Zhang,⁵ Gang Yao,^{6,*}

¹*College of Mathematics and Physics, Leshan Normal University, Leshan 614004, China.*

²*Institute of Atomic and Molecular Physics, Sichuan University, Chengdu 610065, China.*

³*School of New Energy Materials and Chemistry, Leshan Normal University, Leshan 614004, China.*

⁴*Institute of Computer Application, China Academy of Engineering Physics, Mianyang 621900, China.*

⁵*College of Physics and Electronics Information, Yunnan Key Laboratory of Optoelectronic Information Technology, Yunnan Normal University, Kunming, 650500, China.*

⁶*Tsung-Dao Lee Institute, Shanghai Jiao Tong University, Shanghai 200240, China.*

Abstract: Hydrides offer an opportunity to study high-temperature (T_c) superconductivity at experimentally achievable pressures. However, they remained extremely high. Using density functional theory calculations, herein we demonstrated that a newly rare earth hydride, namely bulk ErH₂, could be superconducting with a T_c around 80 K at 14.5 GPa. To date, the driven pressure is the lowest reported value for compressed hydrides. Besides superconductivity, Fermi Surface nesting and Kondo effect were manifested at this pressure. Intriguingly, due to Kondo destruction, superconductivity was prone to exist at 15 GPa. Under the rest of applied pressures, we also revealed a gap of band structure at 20 GPa on the background of normal metallic states. At 20 GPa, this compressed system could act as a host of superconductor being judged from a sharp jump of spontaneous magnetic susceptibility with an evanescent spin density of state at Fermi level along with the competition between spin density wave and superconductivity. Finally, electron pairing glue for ErH₂ at these three typical pressures was attributed to the antiferromagnetic spin fluctuation.

1. Introduction

Hydrogen in certain hydrides can become metallic at a lower pressure than pure hydrogen, presumably because of additive effects from chemical precompression.¹ These hydrides might well be superconducting up to high critical transition temperature (high- T_c). Several theoretical and experimental efforts were underway to better understand the high- T_c superconductivity of such hydrides. These compounds include GeH₄, (64 K at 220 GPa),² YH₃, (40 K at 17.7 GPa),³ H₃S, (203 K at 90 GPa),⁴ VH₈, (71.4 K at 200 GPa),⁵ LaH₁₀, (260 K at 180-200 GPa,⁶ and 250 K at 170 GPa⁷), and other room-temperature superconductors YH₁₀, (303 K at 400 GPa),⁸ Li₂MgH₁₆, (473 K at 250 GPa).⁹ Note that in all the hydrides mentioned above, the major glue for electron pairing is phonon.

Among rare-earth metals, Er showed a powerful getter for hydrogen.¹⁰ The stoichiometry erbium dihydride (ErH₂) and its nonstoichiometric composition ErH_{2+x} ($-0.15 < x < 0.15$) both crystallize with fcc-CaF₂ type crystal structure (space group: $Fm-3m$), which has often been described as the β -Phase.^{11,12} The conventional unit cell of ErH₂ is shown in Fig. 1 in which the H atoms occupied the tetrahedral sites of the Er fcc lattice. In the meantime, the f electrons in lattice are often neither fully localized around their host nuclei nor fully itinerant. This localized versus itinerant duality has proposed the involvement of f electrons as valence ones in the systems, that is, strongly correlated-electron materials, therefore promoting the emerging researches of heavy fermion superconductors.¹³ On the other hand, it was argued that antiferromagnetic (AFM) spin fluctuation was another plausible pairing mechanism driven by Coulomb repulsion in this system, and could lead to high- T_c superconductivity.¹⁴⁻¹⁷ The Hubbard model could be consequently applied to this system.¹⁸⁻²⁰ AFM spin fluctuation could be reflected with mutation from a large Fermi Surface (FS) to a small one,²¹ and a jump of spin DOS at Fermi level (E_F) or spontaneous magnetic susceptibility (χ_s).^{15,17} It is worth investigating whether a compressed system can be superconducting and if there is another pairing mechanism. Despite the investigation discussed above for f electrons in a crystal, a systematic study of possible pressure-induced superconductivity in ErH₂ is still missing.

In this work, we use first-principles approaches to investigate the high- T_c superconductivity of ErH₂, a heavy fermion hydride under pressures. Our purposes were to predict a relatively high T_c at moderate pressure, and to find several accompanying physical behaviors, such as FS nesting, Kondo effect, Kondo destruction and a gap of band structure on the background of normal metallic states under several corresponding typical pressures.

2. Methods

Based on Density Functional Theory (DFT), the present calculations were performed using the Cambridge Serial Total Energy Package (CASTEP) code.²² The exchange and correlation interactions were described by the Generalized Gradient Approximation (GGA) of Perdew and Wang (PW91).²³ Norm-conserving

pseudopotentials of Er and H were taken from the CASTEP library to describe the properties of the perfect crystal. The valence electron configurations of Er and H were $4f^{11}5d^15s^25p^66s^2$ and $1s^1$, respectively. The geometry optimizations of the shape and size of its unit cell were performed using the plane-wave basis sets with energy cutoff of 380 eV, and a $10 \times 10 \times 10$ Monkhorst–Pack (MP) grid sampling the Brillouin Zone (BZ), i.e. k-points which was $36 \times 36 \times 36$ for electronic structure calculations including FSs and Electron Localization Functions (ELFs). Spin polarization was taken into account for all valence electrons. The Hubbard U model for strongly correlated Er- f electrons was considered, and on-site $U = 6$ eV. The phonon calculations were performed using finite displacements method²⁴ with the same precision settings of its geometry optimizations. All above parameter settings and their values were verifiable to convergence tests.

3. Results and discussion

ErH₂ was experimentally confirmed to possess AFM²⁵ that was subjected to have an intimate link with both FS nesting²⁶ and superconductivity.¹⁵ The FS topologies were calculated out in this work accompanying with their electronic Density of States (DOS) and band structures under ambient pressures ranging from 0 to 21.5 GPa.

The band structures under 0, 14.5, 15 GPa and other pressures except 20 GPa were respectively shown in Fig. 2a-d. The results of FSs appeared three types of topology as shown in Fig. 3a-d, electronlike-type under 0 GPa, holelike-type under 14.5 and 15 GPa (large and small respectively) and open-type at other pressures except for 20 GPa under which DOS and band structure revealed a gap, thus showed no FS around its E_F . Compared with 0 GPa, at which the corrugated FS reflected the influence of phonon on the properties of electrons around E_F , the other smooth FSs in Fig. 3 indicated that the interaction between phonon and electrons decreased considerably.²⁷

The topology of the holelike FS at 14.5 GPa (Fig. 3b) did show nesting property which was in accordance with its AFM.²⁵ This consistency between FS nesting and AFM had also been confirmed in the conclusion for cubic structural ErGa₃.²⁶ This FS was apparently the largest one in the whole applied pressures (Fig. 3a-d). Moreover, in the conduction band region at this pressure (Fig. 4c), there was a sharp spin-down f (β) peak between 4-5 eV just corresponding to the spin-up conduction d (α) electrons in this energy scale. Hence, the state at 14.5 GPa (Fig. 3b) could infer the Kondo effect,¹³ in which the fully itinerant f (β) electrons like magnetons immersed in conduction $d(\alpha)$ electrons, entangled with them sufficiently, and contributed to the Fermi volume.^{13,28} This itinerancy of f electrons was also embodied with the localized s electrons of H in the ELF at this pressure (Fig. 4a). Compared with the ELFs under other pressures (Fig. 4b) where electrons localized around Er, the ELF at 14.5 GPa (Fig. 4a) showed a distinct localization of electrons around H. Judging from Fig. 4c in which two large H-derived sharp s electrons DOS peaks (spin-up (α) and spin-down (β) respectively) were most adjacent to the E_F , H were essentially isolated like atomic

H in this lattice. Accordingly, the full formation of a large FS could correspond to heavy fermion superconductivity.²¹ Meanwhile, Fig. 4e demonstrated the variation of spin DOS at E_F and the χ_s along with the applied pressures. Combining with the explicit hopping of spin DOS at E_F at 14.5 GPa without abrupt jump of χ_s (Fig. 4e) and the largest FS with its nesting (Fig. 3b), superconductivity could be implied at 14.5 GPa being mediated by AFM spin fluctuation.¹⁴⁻¹⁷

Fermi Liquid (FL) could easily exist in this state.¹³ Furthermore, basing on phonon calculation, the lattice specific heat at 14.5 GPa was also calculated out.²⁹ The specific heat (C) in the form of C/T dependence on T^2 being shown in Fig. 5 under ambient pressures, was obtained with formula (1):^{30,31}

$$C = \gamma_1 T^3 + \gamma_2 T \quad (1)$$

Here, the first term is lattice specific heat, the second term is electrons contribution. γ_1 is interatomic force constant, $\gamma_2 = \frac{\pi^2}{3} k_B^2 g(E_F)$, $g(E_F)$ is the DOS at E_F , k_B is Boltzmann constant. For FL state, the electrons specific heat depends on T linearly, i.e. $\gamma_2 T$. With these regards, high- T_c superconductivity could be predicted with $T_c = 78.9$ K from the kink point of the curve at 14.5 GPa.²⁷ This T_c value was around boiling point of liquid nitrogen.

In contrast to Kondo effect, superconductivity could also be driven by Kondo destruction transforming from a large FS to a small one in heavy fermion superconductors, such as CeCu_2Si_2 .²¹ The FS of ErH_2 at 15 GPa collapsed abruptly as shown in Fig. 3c which was identified as destruction of Kondo effect.^{13,21,32} Hence, this quantum criticality at 15 GPa could also be prone to possess superconductivity. This phenomenon implied the fully localization of f electrons around their host nuclei, i.e. Er, as the ELF (Fig. 4b) had shown. The fact that the localized f electrons do not contribute to the Fermi volume^{13,28} was consistent with the small FS (Fig. 3c).

Subsequently, with the Kondo destruction (Fig. 3c), the Ruderman-Kittel-Kasuya-Yosida (RKKY) interaction played a dominant role that led to the crossover feature from FL at 14.5 GPa to Non-Fermi-Liquid (NFL) behavior at 15 GPa where the indirect interaction among the localized f electrons with magnetic moments was mediated mainly by the conduction d electrons.^{13,21} The DOS was shown in Fig. 4d. Therefore, despite the superconductivity as it was predicted at 15 GPa, the dependence of electrons specific heat on T was nonlinear,^{30,31} so the T_c value at 15 GPa could not be obtained from the kink point of the C/T versus T^2 curve in Fig. 5. This superconductivity could also be inferred with the medium of AFM spin fluctuation from the noticeable hopping of spin DOS at E_F between 14.5 and 15 GPa without steep variation of χ_s in this pressure region (Fig. 4e) as well as this FS jump.¹⁴⁻¹⁷ The accompanying behaviors which could also to some extent support the affirmation of superconductivity at 15 GPa were presented in the Supplemental Material.³³

As it can be prominently seen in DOS and band structures of this bulk (Fig. 6a-c), there was a gap of 6.6 eV at 20 GPa in the present calculations on the background of normal metallic states under the rest of applied pressures. It could be seen in Fig. 6b that the itinerant electrons were from s electrons of H and s, p, d ones of Er, whose all spin with up and down direction had almost the same weight and symmetric distribution. The fully localized electrons were from f electrons of Er as shown in the ELF (Fig. 4b) and the DOS (Fig. 6b). This manifested that itinerant AFM at 20 GPa vanished abruptly, leading to a localized AFM insulating state.³⁴ This transition resulted in a sharp jump of χ_s and an evanescent spin DOS at E_F (Fig. 4e) exclusively at this pressure which could also signify an AFM spin fluctuation. This bulk under 20 GPa could thus act as a host of superconductor owing to this pairing glue.¹⁴⁻¹⁷ This implication was supported by the competition between Spin Density Wave (SDW) and superconductivity.^{13,35-37} The existence of SDW could be determined with Pauli paramagnetic susceptibility ($\chi_P(0)$) which was expressed as follow:³⁴

$$\chi_P(0) = 2\mu_B^2\mu_0g(E_F) \quad (2)$$

Where, μ_B is Bohr magneton, μ_0 is vacuum permeability, $g(E_F)$ is the DOS at E_F . The SDW was suppressed from the zero DOS at E_F (Fig. 6b) and the formula (2). This hypothesis could also be supported by the tiny and clear deviation of the V/V_0 versus pressures relation calculated directly with DFT at this pressure away from the monotonous trend of the curve fitted with $E-V$ data of this work (see Fig. S1 in the Supplemental Material³³). The DOS (Fig. 6b) displayed that the hybridization between localized f moments and itinerant electrons is very weak. This could infer the NFL behavior at this pressure.^{13,36} Meanwhile, as shown in Fig. 6a and c, the band structures of (110) surface of this bulk at 20 GPa with the range from -6 to 6 eV exhibiting metallic, came very within the gap of this bulk. This metallic surface state with bulk insulating state emerged also in the archetype Kondo insulator, i.e. SmB₆.³² Our results could postulate a possibility for topological superconductor which could host Majorana Zero Mode.^{38,39}

4. Conclusion

In summary, we revealed that superconductivity emerged in ErH₂ under moderate pressures which were 14.5, 15 and 20 GPa with DFT calculations. We proposed that ErH₂ at 14.5 GPa was a potential high- T_c superconductor whose T_c was around 80 K. Our current result of the gapped bulk state with metallic surface state at 20 GPa could be conducive to the exploration of topological superconductor which will stimulate further experimental and theoretical studies for the feasibility of ErH₂ to host Majorana Zero Mode.

Corresponding Author

*E-mail: yaogang1257@sjtu.edu.cn

ORCID

Yiding Liu: 0000-0003-2265-1827

Gang Yao: 0000-0002-4944-4118

Notes

The authors declare no competing financial interest.

Acknowledgements

This work was supported by the National Natural Science Foundation of China (Grant No. 12104294). This work was carried out at Shanxi Supercomputing Center of China, and the calculations were performed on TianHe-2.

References

- (1) Ashcroft N. W., Hydrogen dominant metallic alloys: high temperature superconductors? *Phys. Rev. Lett.* (2004);92: 187002.
- (2) Gao G., Oganov A. R., Bergara A., Martinez-Canales M., Cui T., Iitaka T., Ma Y., and Zou G., Superconducting high pressure phase of germane. *Phys. Rev. Lett.* (2008);101: 107002.
- (3) Kim D. Y., Scheicher R. H., and Ahuja R., Predicted High-Temperature Superconducting State in the Hydrogen-Dense Transition-Metal Hydride YH_3 at 40 K and 17.7 GPa. *Phys. Rev. Lett.* (2009);103: 077002.
- (4) Drozdov A. P., Eremets M. I., Troyan I. A., Ksenofontov V., and Shylin S. I., Conventional superconductivity at 203 kelvin at high pressures in the sulfur hydride system. *Nature (London)* (2015);525: 73.
- (5) Li X. and Peng F., Superconductivity of pressure-stabilized vanadium hydrides. *Inorg. Chem.* (2017);56: 13759-13765.
- (6) Somayazulu M., Ahart M., Mishra A. K., Geballe Z. M., Baldini M., Meng Y., Struzhkin V. V., and Hemley R. J., Evidence for Superconductivity above 260 K in Lanthanum Superhydride at Megabar Pressures. *Phys. Rev. Lett.* (2019);122: 027001.
- (7) Drozdov A. P. *et al.*, Superconductivity at 250 K in lanthanum hydride under high pressures. *Nature (London)* (2019);569: 528-531.
- (8) Peng F., Sun Y., Pickard C. J., Needs R. J., Wu Q., and Ma Y., Hydrogen clathrate structures in rare earth hydrides at high pressures: possible route to room-temperature superconductivity. *Phys. Rev. Lett.* (2017);119: 107001.
- (9) Sun Y., Lv J., Xie Y., Liu H., and Ma Y., Route to a Superconducting Phase above Room Temperature in Electron-Doped Hydride Compounds under High Pressure. *Phys. Rev. Lett.* (2019);123: 097001.
- (10) Yang L., Peng S., Long X., Gao F., Heinisch H. L., Kurtz R. J., and Zu X. T., Ab initio study of intrinsic, H, and He point defects in hcp-Er. *J. Appl. Phys.* (2010);107: 054903.
- (11) Bonnet J. and Daou J., Rare-earth dihydride compounds: Lattice thermal expansion and investigation of the thermal dissociation. *J. Appl. Phys.* (1977);48: 964-968.

- (12) Wixom R. R., Browning J. F., Snow C. S., Schultz P., and Jennison D. R., First principles site occupation and migration of hydrogen, helium, and oxygen in β -phase erbium hydride. *J. Appl. Phys.* (2008);103: 123708.
- (13) Gegenwart P., Si Q., and Steglich F., Quantum criticality in heavy-fermion metals. *Nat. Phys.* (2008);4: 186.
- (14) Ikeda H., Suzuki M.-T., and Arita R., Emergent Loop-Nodal S-Wave Superconductivity in CeCu_2Si_2 : Similarities to the Iron-Based Superconductors. *Phys. Rev. Lett.* (2015);114: 147003.
- (15) Nakai Y., Iye T., Kitagawa S., Ishida K., Kasahara S., Shibauchi T., Matsuda Y., Ikeda H., and Terashima T., Normal-state spin dynamics in the iron-pnictide superconductors $\text{BaFe}_2(\text{As}_{1-x}\text{P}_x)_2$ and $\text{Ba}(\text{Fe}_{1-x}\text{Co}_x)_2\text{As}_2$ probed with NMR measurements. *Phys. Rev. B* (2013);87: 174507.
- (16) Pines D., Finding new superconductors: The spin-fluctuation gateway to high T_c and possible room temperature superconductivity. *J Phys. Chem. B* (2013);117: 13145-13153.
- (17) Moriya T. and Ueda K., Antiferromagnetic spin fluctuation and superconductivity. *Rep. Prog. Phys.* (2003); 66: 1299–1341.
- (18) Anisimov V. I., Zaanen J., Andersen O.K., Band theory and Mott insulators: Hubbard U instead of Stoner I. *Phys. Rev. B.* (1991); 44: 943-954.
- (19) Dudarev S. L., Botton G. A., Savrasov S. Y., Humphreys C. J., Sutton A. P., Electron-energy-loss spectra and the structural stability of nickel oxide: An LSDA+U study. *Phys. Rev. B.* (1998); 57: 1505-1509.
- (20) Cococcioni M., de Gironcoli S., Linear response approach to the calculation of the effective interaction parameters in the LDA+U method. *Phys. Rev. B.* (2005); 71: 035105.
- (21) Si Q. and Paschen S., Quantum phase transitions in heavy fermion metals and Kondo insulators. *Phys. Status. Solidi. B* (2013);250: 425-438.
- (22) Segall M., Lindan P. J., Probert M. a., Pickard C. J., Hasnip P. J., Clark S., and Payne M., First-principles simulation: ideas, illustrations and the CASTEP code. *J. Phys.: Condens. Matter* (2002);14: 2717.
- (23) Perdew J. P., Chevary J. A., Vosko S. H., Jackson K. A., Pederson M. R., Singh D. J., and Fiolhais C., Atoms, molecules, solids, and surfaces: Applications of the generalized gradient approximation for exchange and correlation. *Phys. Rev. B* (1992);46: 6671-6687.
- (24) Montanari B. and Harrison N. M., Lattice dynamics of TiO_2 rutile: influence of gradient corrections in density functional calculations. *Chem. Phys. Lett.* (2002);364: 528-534.
- (25) Vajda P. and Daou J., Magnetic and metal-semiconductor transitions in ordered and disordered $\text{ErH}(\text{D})_{2+x}$. *Phys. Rev. B* (1994);49: 3275.
- (26) Biasini M., Ferro G., Kontrym-Sznajd G., and Czopnik A., Fermi surface nesting and magnetic structure of ErGa_3 . *Phys. Rev. B* (2002);66: 075126.
- (27) Charles Kittel., *Introduction to Solid State Physics.* (8th Edition). John Wiley & Sons Inc. New Jersey (2004).
- (28) Hoshino S. and Kuramoto Y., Itinerant versus localized heavy-electron

- magnetism. Phys. Rev. Lett. (2013);111: 026401.
- (29) Baroni S., de Gironcoli S., dal Corso A., and Giannozzi P., Phonons and related crystal properties from density-functional perturbation theory. Rev. Mod. Phys. (2001);73: 515-562.
- (30) Settai R., Takeuchi T., and Ōnuki Y., Recent Advances in Ce-Based Heavy-Fermion Superconductivity and Fermi Surface Properties. J. Phys. Soc. Jpn. (2007);76: 051003.
- (31) Kittaka S., Aoki Y., Shimura Y., Sakakibara T., Seiro S., Geibel C., Steglich F., Ikeda H., and Machida K., Multiband superconductivity with unexpected deficiency of nodal quasiparticles in CeCu₂Si₂. Phys. Rev. Lett. (2014);112: 067002.
- (32) Zhou Y. *et al.*, Quantum phase transition and destruction of Kondo effect in pressurized SmB₆. Sci. Bull. (2017);62: 1439-1444.
- (33) See Supplemental Material for supporting information of the hypotheses of superconductivity of ErH₂ at 15 and 20 GPa.
- (34) Feng D. and Jin G.-J., Condensed Matter Physics (Vol.1). Higher Education Press. Beijing (2012); in Chinese.
- (35) Subedi A., Zhang L., Singh D. J., and Du M.-H., Density functional study of FeS, FeSe, and FeTe: Electronic structure, magnetism, phonons, and superconductivity. Phys. Rev. B (2008);78: 134514.
- (36) G. F. Chen., Z. Li., D. Wu., G. Li., W. Z. Hu., J. Dong., P. Zheng., J. L. Luo., and N. L. Wang., Superconductivity at 41K and its competition with Spin-Density-Wave instability in layered CeO_{1-x}F_xFeAs. Phys. Rev. Lett. (2008); 100: 247002.
- (37) J. Dong., H. J. Zhang., G. Xu., Z. Li., G. Li., W. Z. Hu., D. Wu., G. F. Chen., X. Dai., J. L. Luo., Z. Fang., and N. L. Wang., Competing orders and spin-density-wave instability in La(O_{1-x}F_x)FeAs. Euro. Phys. Lett. (2008); 83: 27006.
- (38) Sun H.-H. *et al.*, Majorana Zero Mode Detected with Spin Selective Andreev Reflection in the Vortex of a Topological Superconductor. Phys. Rev. Lett. (2016);116: 257003.
- (39) Ran S. *et al.*, Nearly ferromagnetic spin-triplet superconductivity. Science (2019);365: 684-687.

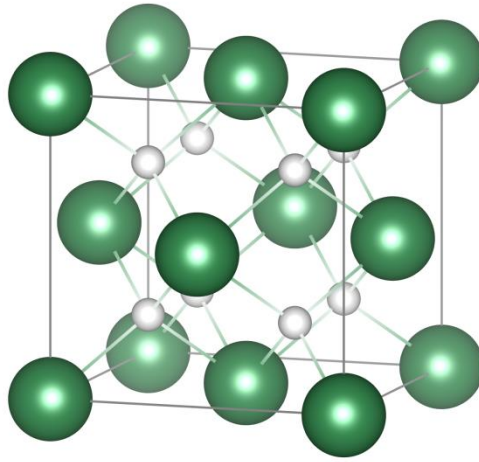


Figure 1. A unit cell of ErH_2 crystal was displayed. The larger green atoms represented the erbium fcc lattice. The eight smaller gray atoms represented hydrogen occupying all of the tetrahedral sites.

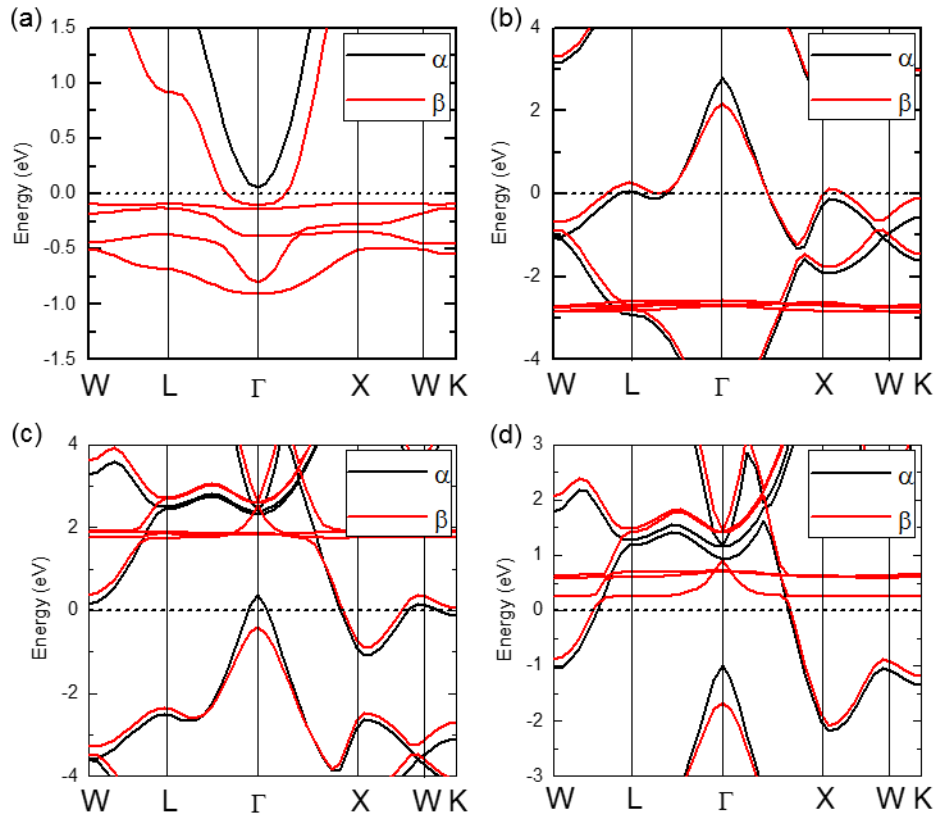


Figure 2. Band structures of ErH_2 under ambient pressures ranging from 0 to 21.5 GPa. (a) 0 GPa, (b) 14.5 GPa, (c) 15 GPa, (d) 0.5 GPa. At the rest of this pressure range except 20 GPa, band structures were similar with (d), α and β denoted spin up and down respectively.

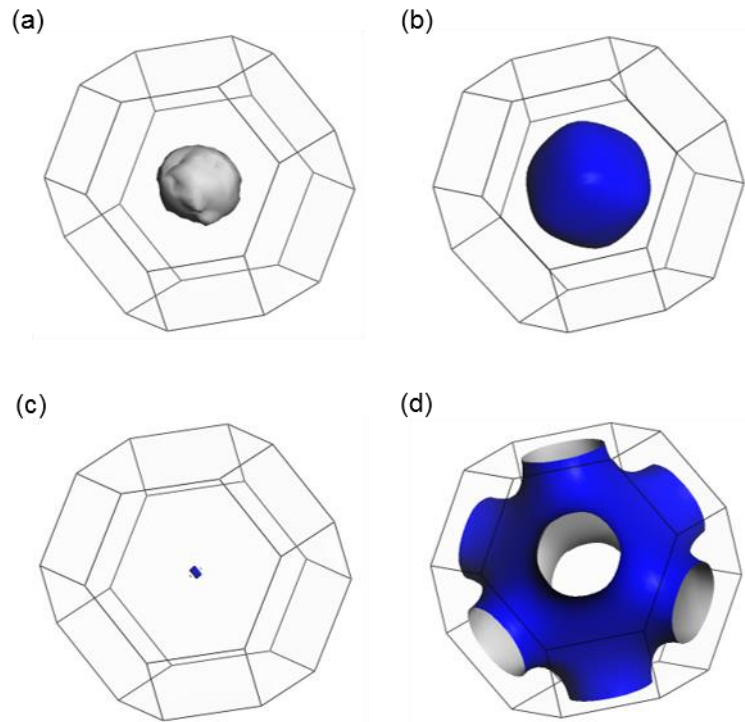


Figure 3. Types of FSs for ErH_2 at ambient pressures ranging from 0 to 21.5 GPa. (a) electronlike-type under 0 GPa. (b), (c) holelike-type at 14.5 and 15 GPa respectively. (d) open-type at 0.5 GPa. At the rest of this pressure range except 20 GPa, the FSs were open-type similar with the one at 0.5 GPa.

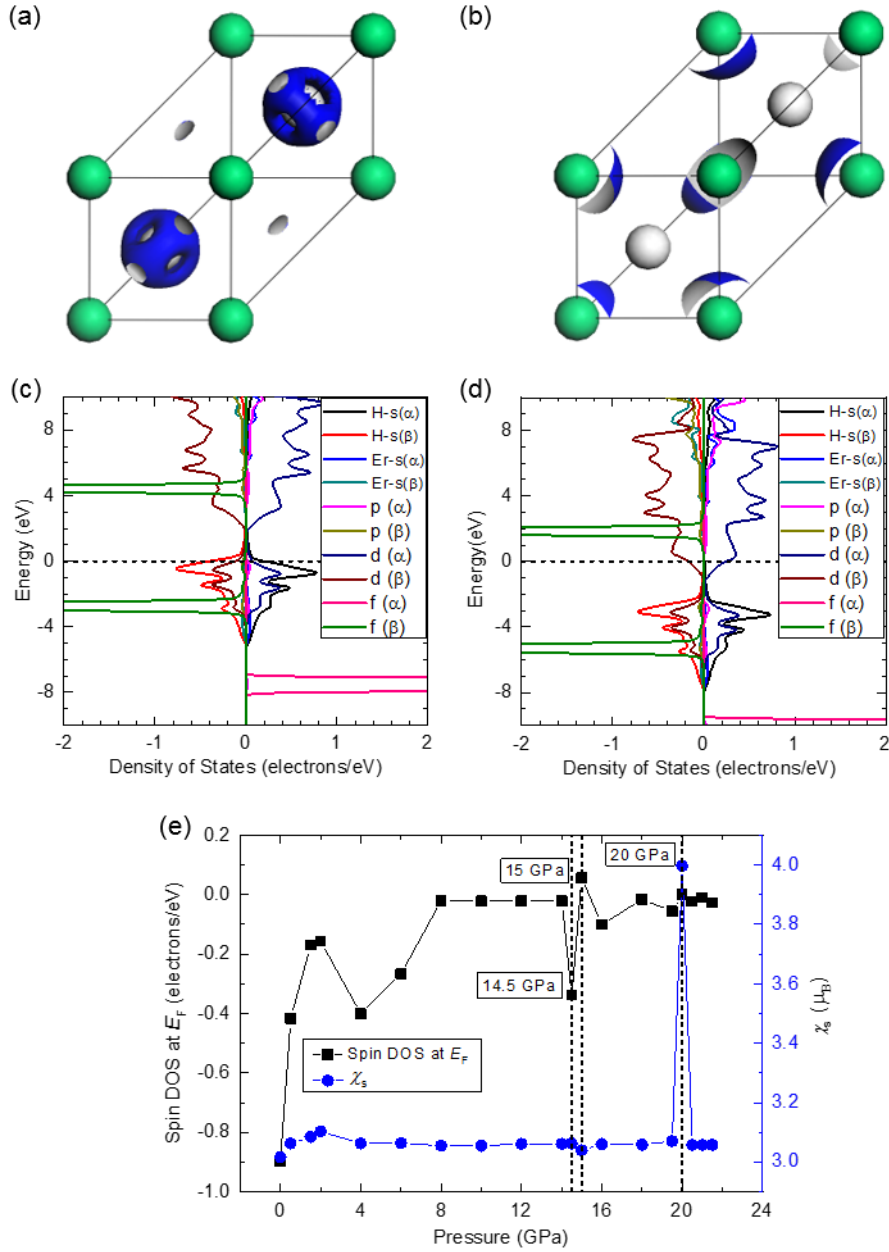


Figure 4. (a) Schematic diagram of Electron Localization Function (ELF) at 14.5 GPa. (b) The ELF's under other pressures of the whole applied pressures. The primitive cell of ErH₂ crystal were displayed. Green spheres represented Er, while gray spheres represented H. (c) and (d) The DOS at 14.5 and 15 GPa respectively. (e) The variation of spin DOS at E_F and the spontaneous magnetic susceptibility (χ_s) along with the applied pressures.

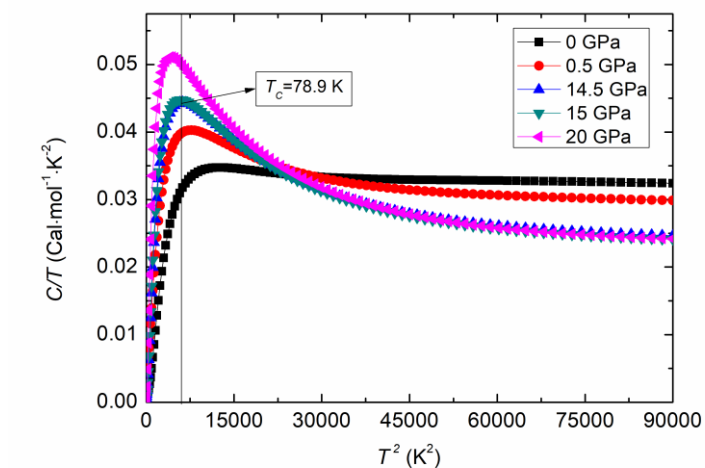


Figure 5. T^2 dependence of the specific heat in the form of C/T under ambient pressures for ErH_2 .

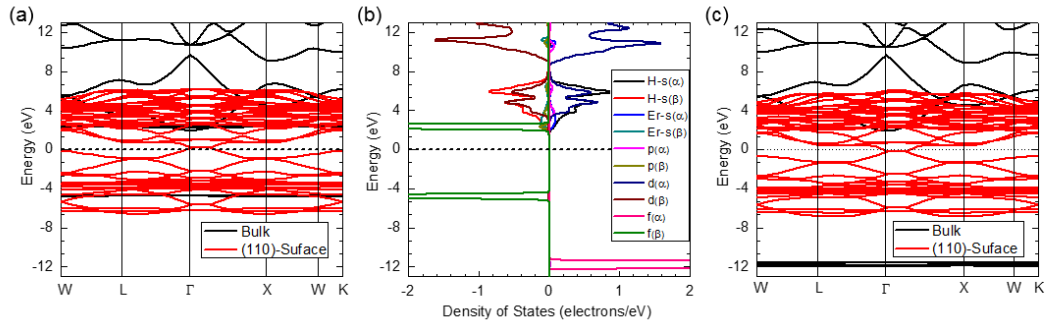


Figure 6. (a) and (c) The band structures of this bulk at 20 GPa with electronic spin down and up respectively. The band structures of (110) surface being built with $1 \times 2 \times 1$ supercell of this bulk at 20 GPa were also plotted with red color in (a) and (c). The energy scales of this metallic surface state were from -6 to 6 eV. (b) The DOS of this bulk at 20 GPa. α and β denoted spin up and down respectively.

Supplemental Material for “Predicted high-temperature superconductivity in rare earth hydride ErH₂ at moderate pressure”

Yiding Liu,^{1,2} Qiang Fan,³ Jianhui Yang,¹ Lili Wang,⁴ Weibin Zhang,⁵ Gang Yao,^{6,*}

¹College of Mathematics and Physics, Leshan Normal University, Leshan 614004, China.

²Institute of Atomic and Molecular Physics, Sichuan University, Chengdu 610065, China.

³School of New Energy Materials and Chemistry, Leshan Normal University, Leshan 614004, China.

⁴Institute of Computer Application, China Academy of Engineering Physics, Mianyang 621900, China.

⁵College of Physics and Electronics Information, Yunnan Key Laboratory of Optoelectronic Information Technology, Yunnan Normal University, Kunming, 650500, China.

⁶Tsung-Dao Lee Institute, Shanghai Jiao Tong University, Shanghai 200240, China.

*yaogang1257@sjtu.edu.cn

The accompanying behaviors which could also to some extent support the affirmation of superconductivity at 15 GPa were presented in this Supplemental Material. The calculated elastic constants C_{ij} under ambient pressures were presented in Table S1. Judged from the mechanical stability criterion,¹ this bulk became mechanical unstable at 14.5 GPa and up to 21.5 GPa except 15 GPa, as shown in Table S1. When the applied pressure was higher than 21.5 GPa, this bulk became lattice dynamical unstable, i.e. imaginary frequency of phonon dispersions (not show) which was also the reason why the upper limit of the applied pressure in this work was 21.5 GPa. The mechanical stability criterion for cubic crystal could be expressed as:¹ $\tilde{C}_{44} > 0$, $\tilde{C}_{11} > |\tilde{C}_{12}|$, $\tilde{C}_{11} + 2\tilde{C}_{12} > 0$, where $\tilde{C}_{\alpha\alpha} = C_{\alpha\alpha} - P$ ($\alpha = 1, 4$) and $\tilde{C}_{12} = C_{12} + P$, where P is the applied pressure. Meanwhile, superconductivity could also be reflected by an anomalous elastic softening over a temperature range for PuCoGa₅ which was a heavy fermion superconductor with $T_c = 18.5$ K.² Then, the analogous hopping of mechanical stability between 14.5 and 15 GPa of ErH₂ (Table S1) could also support the deduction of superconductivity at 15 GPa.

By means of Birch–Murnaghan Equation of State (EOS) fitting, the normalized molar volume (V/V_0) of ErH₂ at 300 K as a function of pressures (Fig. S1) was obtained by GIBBS thermodynamics scheme³ using single point energy of unit cell (E) versus its volume (V) within DFT, i.e. E - V curve which could be produced in this work (Fig. S2). The corresponding V/V_0 versus pressures relation calculated directly

with DFT of this work was also plotted in Fig. S1. There was a tiny and clear deviation at this pressure away from the monotonous trend of the fitted curve in this work. Both the E - V data and the V/V_0 versus pressures relation of DFT had the same parameter settings and precision with the geometry optimizations of its unit cell (see **2. Methods** of the main text). The comparison with experimental data for $\text{ErH}_{2.091}$ and $\text{ErH}_{1.95}$ measured at room temperature using diamond anvil cell techniques (DAC)⁴ was also shown in Fig. S1.

The hypothesis of superconductivity at 20 GPa could also be supported by the tiny and clear deviation of the V/V_0 versus pressures relation calculated directly with DFT at this pressure away from the monotonous trend of the curve fitted with E - V data of this work (see Fig. S1).

References

- (1) Sin'Ko G. and Smirnov N., Ab initio calculations of elastic constants and thermodynamic properties of bcc, fcc, and hcp Al crystals under pressure. *J. Phys.: Condens. Matter* (2002);14: 6989.
- (2) Ramshaw B., Shekhter A., McDonald R. D., Betts J. B., Mitchell J., Tobash P., Mielke C., Bauer E., and Migliori A., Avoided valence transition in a plutonium superconductor. *Proc. Natl. Acad. Sci. U.S.A.* (2015);112: 3285-3289.
- (3) Blanco M., Francisco E., and Luana V., GIBBS: isothermal-isobaric thermodynamics of solids from energy curves using a quasi-harmonic Debye model. *Comput. Phys. Commun.* (2004);158: 57-72.
- (4) Palasyuk T., Tkacz M., and Vajda P., High pressure studies of the erbium–hydrogen system. *Solid. State. Commun.* (2005);135: 226-231.

Supplemental Figures

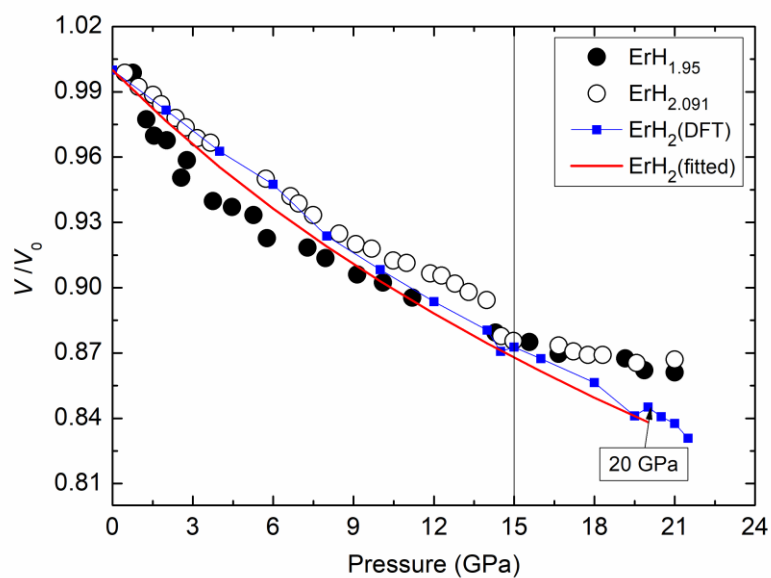


Fig. S1 The fitted normalized molar volumes (V/V_0) as a function of pressures for ErH₂ at 300 K (red solid line) using GIBBS thermodynamics scheme³ with E - V data of DFT in this work. The corresponding relation calculated directly with DFT of this work was also plotted (blue solid line with square). The DAC data from Ref. 4 measured at room temperature for ErH_{1.95} (solid circle) and ErH_{2.091} (hollow circle) were also shown with denotation in the inset.

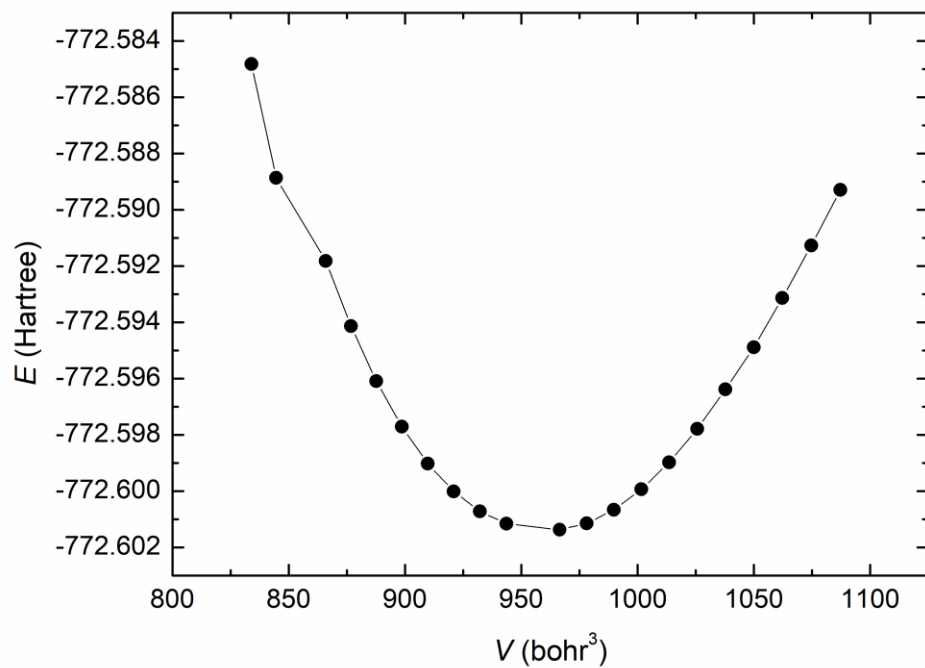


Fig. S2 The single point energy for unit cell (E) of ErH_2 versus its volume (V) within DFT.

Supplemental Table

Table S1. The calculated elastic constants C_{ij} of ErH₂ under ambient pressures (in GPa) and the satisfaction with mechanical stability criteria (Y and N denoted the satisfaction and the unsatisfaction respectively).

P	C_{11}	C_{12}	C_{44}	Y/N
0	121.637	51.209	64.972	Y
6	158.495	59.177	54.465	Y
12	133.738	108.377	113.144	Y
14	145.060	101.757	253.158	Y
14.5	127.776	161.299	192.400	N
15	164.900	103.873	119.387	Y
16	148.068	126.347	76.245	N
18	176.988	105.421	-50.332	N
20	129.393	192.898	-24.491	N